Surface Structural Studies of Methanesulfonic Acid at Air /Aqueous Solution Interfaces Using Vibrational Sum Frequency Spectroscopy†

Heather C. Allen,‡ Elizabeth A. Raymond, and Geraldine L. Richmond*

Department of Chemistry, University of Oregon, Eugene, Oregon 97403

Received: September 15, 2000; In Final Form: November 28, 2000

Atmospheric gas phase species such as methanesulfonic acid (MSA) are adsorbed and accommodated into atmospheric aqueous-phase aerosols, and in some cases MSA is thought to be produced via aerosol surface chemistry. The studies described herein probe the surface molecular structure of MSA at aqueous solution surfaces using surface vibrational sum frequency spectroscopy (VSFS). In the studies presented here, it is shown that MSA partitions to the surface and that the surface MSA has a preferred orientation in which the methyl group points away from the liquid surface. The surrounding surface water structure is significantly affected by the adsorption of MSA. Small amounts of MSA at the surface of water cause the water molecule vibrational stretching modes to shift to lower energies. This shift is indicative of stronger coupling between the water molecules caused by the presence of MSA. Additional VSF studies show that MSA is effectively displaced by sulfuric acid at an aqueous surface. The structural details presented here may have implications for understanding atmospheric aerosol growth properties.

Introduction

Understanding the adsorption and molecular structure of methanesulfonic acid, MSA (CH_3SO_3H), at an aqueous solution surface is important because of the role MSA plays in tropospheric aerosol (liquid and solid particle) chemistry. In addition, studies elucidating MSA surface structure have particular relevance to the understanding of past and future global climate change. Ice core measurements of MSA and non sea-salt sulfate (NSS) concentrations, and MSA:NSS ratios have been used by glaciologists to help understand historical climate trends. An inverse relationship between glacially deposited MSA (originating from the atmosphere) and planetary temperatures has been shown to exist.[1] In addition to resolving past long-term climate trends, understanding the causal relationships that shape current climate trends is important to the understanding of global climate change. Tropospheric aerosols have been recognized to alter climate by changing the albedo of the atmosphere.[2−4] Tropospheric aerosols are formed by aerosol nucleation, growth, and chemical processes in which MSA and NSS are important factors. Therefore, understanding heterogeneous chemical processes is necessary to the understanding of climate change.[5]

In this paper, we present studies of the adsorption and molecular structure of MSA at neat and aqueous solution surfaces. The structure of surface-adsorbed MSA is explored as well as how that structure changes as a function of concentration in binary aqueous and ternary sulfuric acid aqueous solutions. The average orientation of surface MSA has been measured to help understand the factors that influence the resulting surface water structure. Additionally, measurements examining how the structure and hydrogen bonding of surface water change upon addition of MSA and MSA/sulfuric acid have been made. We find that the hydrogen bonding and free OH modes of surface water are both affected by the presence of surface MSA.

Surface vibrational sum frequency spectroscopy (VSFS) is the primary technique employed in these studies. The surface specificity of this second-order nonlinear optical method allows the vibrational spectrum of methanesulfonic acid adsorbed on a water surface to be obtained. This surface sensitivity arises from the noncentrosymmetric nature of the interface that gives rise to a second-order nonlinear response, i.e., sum frequency, difference frequency, and second harmonic generation. Recent advances in instrumentation used for VSFS measurements, in particular the use of picosecond and femtosecond[6] pulse widths, have resulted in higher nonlinear efficiencies that lessen the risk of surface damage.[7] By increasing the nonlinear efficiencies, small surface coverage and weak vibrational modes that were below VSFS detection limits for a gas/liquid interface are now more easily observed. In our laboratory these advances and improvements in detection have opened new opportunities for studying atmospheric processes. Our improved spectral resolution, methods for spectral analysis that include the phase of the VSFS response, and increased sensitivity to submonolayer coverages of atmospherically relevant molecules have made the studies reported herein possible.

Experimental Section

The laser system used in these studies has been previously described.[8,9] A summary of the experimental setup and recent modifications of this system are detailed below. The production of the 800 nm beam (kHz repetition rate, 2 ps, 1.6 W) begins with a Ti:sapphire (Coherent Mira) passively mode-locked laser pumped with 5.5 W of a 532 nm laser beam from a Coherent Verdi laser. The Mira produces an ∼135 fs, 800 nm seed, which is stretched in time to ∼100 ps and amplified with a Quantronix regenerative amplifier and a double pass Ti:sapphire amplifier,

† Part of the special issue "Harold Johnston Festschrift".

* To whom correspondence should be addressed.

‡ Postdoctoral fellow for the NOAA Postdoctoral Program in Climate and Global Change. Current address: Department of Chemistry, The Ohio State University, 100 W. 18th Ave., Columbus, OH 43210.

10.1021/jp0032964 CCC: $20.00
Published on Web 12/30/2000

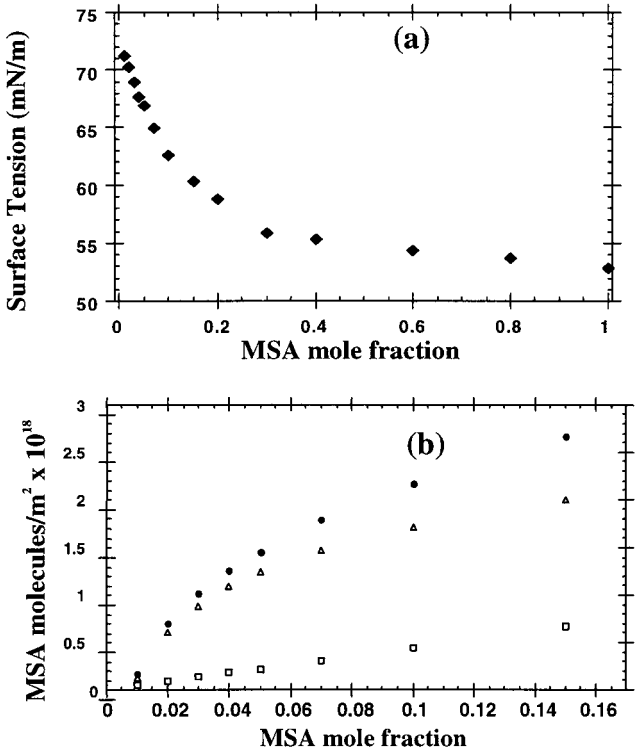

Figure 1. (a) Surface tension measurements of aqueous MSA solutions. (b) Two-dimensional bulk density (□), Gibbs surface excess (△), and surface number density (●) of aqueous MSA solutions. The surface of MSA aqueous solutions, particularly at low concentrations, is enriched in MSA relative to the bulk MSA concentration.

then compressed to 2 ps. The amplifiers are pumped with a total of 12 W of a 527 nm kHz YLF laser. The resulting amplified 800 nm laser beam is split by a 75/25 beam splitter. Approximately 25% of the 800 nm light is used as one of two beams incident at the surface.

The infrared (2700−4000 cm^{-1}) is produced from 75% of the 1.6 W 800 nm beam via a home-built optical parametric amplifier (OPA) system. The OPA consists of two angle-tuned KTP (potassium titanyl phosphate) crystals. Recent changes to this system from previous work[8,9] include the incorporation of a 2 cm length MgO:$LiNbO_3$ crystal that is used as the optical parametric generator (OPG) from which the resultant 1−1.2 μm wavelengths are used to seed the first KTP crystal. We employ a grating for the selection of the seed wavelength. The infrared is generated by seeding the first KTP crystal and then amplifying through the second KTP crystal. Each KTP crystal is pumped with ∼0.425 mJ of the 800 nm beam. The resultant infrared frequencies are scanned as a function of time. The 800 nm beam, focused approximately 1 cm before the interface (∼0.5 mm spot size at the interface), and the infrared beam, focused to ∼0.3 mm at the interface, are temporally and spatially overlapped at the solution surface. The 800 nm and infrared beams are incident at ∼56° and 67° from the surface normal, respectively, in a copropagating geometry. The reflected sum of the two incident frequencies (at ∼ 630 nm) is detected with a cooled CCD camera (Princeton Instruments) after spatial filtering and use of polarization and wavelength selection optics. Spectra are normalized by dividing the SF intensity by the incident infrared energy, which takes into account the changes in infrared intensity as a function of wavelength. In all regions of the spectrum, calibration of a monochromator with different order HeNe lines preceded the calibration of the spectrum by the monochromator.

The intensity of the SF is proportional to the square of the orientationally averaged molecular number density in the interfacial region. Resonant SF intensity is generated at an interface when the infrared frequency is resonant with a Raman and infrared-active vibrational mode of a molecule in the interfacial region. Since VSF is a coherent process, the SF response from vibrational modes of nearby frequencies can constructively, and in some cases, destructively interfere with one another. Spectra presented here were obtained using the SSP and SPS polarization combinations (e.g., SSP: S polarized SF, S polarized 800 nm beam, and P polarized infrared beam). The SSP polarization combination provides data on surface IR-active vibrational modes that have components of their transition moments parallel to the surface normal and the isotropic Raman response from the interface. The SPS polarization combination provides data on surface IR-active modes with transition moment components parallel to the surface plane and the anisotropic Raman response.

Presented spectra were taken at room temperature (∼293 K). Fresh samples are examined for each VSF spectrum taken to minimize atmospheric contamination during the 15 min. scans. We find that experiments conducted under these conditions produce VSFS data identical to what we obtain with the water in an enclosed and N_2 purged cell.

Water used in the experiments is Aldrich HPLC grade (data is identical using Nanopure 18 MΩ H_2O). ACS + grade methane sulfonic acid, 99%, and sulfuric acid, 96+ % solutions were obtained from Aldrich. Surface tension was measured using the Wilhelmy plate method and has been described previously.[10]

Results and Discussion

This section is organized in the following manner. Surface tension data of MSA aqueous solutions are discussed in subsection I to determine surface MSA concentration for various bulk MSA concentrations. Subsection II describes the VSF spectrum of neat water prior to addition of MSA. This is followed in subsection III by the VSF results of these surfaces with different MSA/water mixtures. In subsection IV, VSF spectra of concentrated sulfuric acid, binary, and ternary solutions are compared. This includes SSP VSF spectra of MSA/water solutions, and MSA/sulfuric acid (SA)/water solutions which are discussed in terms of surface displacement and preferential surface species.

I. Surface Tension Measurements of Aqueous MSA Solutions. To understand the surface adsorption properties of aqueous MSA solutions, the surface tension of MSA has been studied as a function of MSA concentration in water. In Figure 1, a and b, measured surface tension (0−1.0 mf MSA; mf = mole fraction) and calculated number densities are plotted versus mole fraction of MSA in water. The 2-dimensional bulk density is calculated from the density of MSA ($\rho^{2/3}$) in order to compare it with the MSA surface excess, which is also in units of molecules/m^2. The surface excess of MSA is the calculated number of molecules in excess compared to the bulk density. The MSA surface number density is the bulk density added to the surface excess.[10] We have used mole fraction values to calculate surface excess due to the lack of published activity data for MSA. Figure 1a shows that the surface tension decreases with increasing bulk MSA concentration. The surface tension does not change significantly beyond 0.3 mf MSA. Figure 1b displays MSA bulk number densities, MSA surface excess and the MSA surface number densities in the low concentration regime. These values have been determined using the surface tension data of Figure 1a and the Gibbs equation. A nearly linear

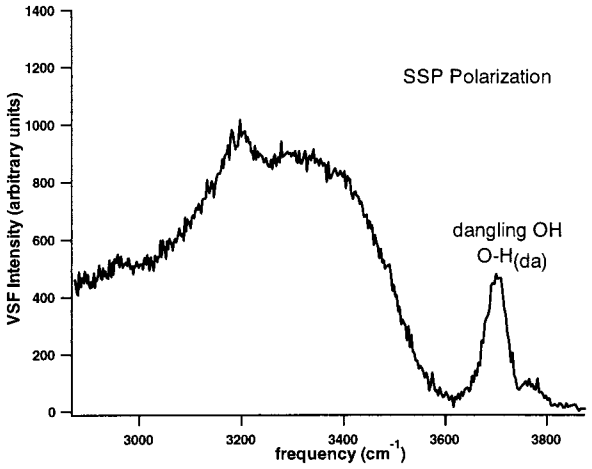

Figure 2. SSP VSF spectrum of the surface of neat water. The broad hydrogen-bonding band extends from below 2900 cm^{-1} to ~3550 cm^{-1}. The dangling OH (free OH) and the gas phase AS are observed at 3702 and 3760 cm^{-1}, respectively.

increase is observed for the bulk number density as a function of MSA mole fraction. In contrast, the surface excess and the surface number density are observed to increase steeply at the low concentrations with a slower increase observed at higher concentrations.

The results of Figure 1b indicate a strong partitioning of MSA to the surface. MSA surface number densities are 7.7 and 7.9 times higher than their corresponding bulk densities at 0.02 and 0.03 mf MSA, respectively. At 0.02 mf MSA and at 0.03 mf MSA the effective surface concentration is 0.15 mf_e MSA and 0.24 mf_e MSA, respectively. In a bulk 0.03 mf MSA solution this translates into 24 MSA to 75 water molecules at the surface (surface ratio of ~1:3) whereas in the bulk there are 3 MSA molecules for every 97 water molecules (bulk ratio of 1:32). At bulk concentrations of 0.1 mf MSA (bulk ratio of 1:9) the magnitude of the difference between bulk and surface concentrations begins to decrease. At this concentration the surface number density is only 5 times higher, giving a surface mf_e of 0.5 (surface ratio of 1:1). The MSA surface population exceeds the surface water population for bulk concentrations greater than 0.10 mf MSA.

Adsorbed organic solutes decrease the surface tension of water. Although highly soluble organic solutes can moderate this effect, these molecules can still partition effectively to the surface of an aqueous solution. Previous surface tension studies of dimethyl sulfoxide (DMSO) show significant surface partitioning of DMSO from aqueous solutions.[10] This was attributed largely to the nonpolar methyl groups that prefer the surface region over the highly polar aqueous phase.[11] Methyl (and methylene) groups do not induce strong hydrogen bonding, therefore, it is more thermodynamically favorable for a molecule at an air/aqueous interface to have its hydrophobic moiety protruding into the air phase of the interfacial region, while the hydrophilic group (e.g., SO_3H group of MSA) is solvated by the H_2O. We conclude that this gives rise to the surface partitioning characteristics that have been observed here for MSA.

II. VSF of the Vapor/Water Interface. To understand how the adsorption of MSA alters the hydrogen bonding of water at the air/water interface, it is first necessary to examine the VSF spectrum of water at a neat air/water interface. Although the VSF spectrum of the air/water interface has been measured in previous studies,[12−22] new insights are provided in these studies that justify acknowledgment. Figure 2 shows the VSF spectrum of surface water taken from HPLC-grade water (pH = 6.5) using SSP polarization. The spectral assignments for the OH stretching modes of bulk liquid water continue to be somewhat controversial due to the broadness of the peaks in the bulk liquid. Thus, we assign our intensity regions for the VSF surface spectrum with some caution and utilize the most acceptable IR and Raman assignments from bulk water measurements. The surface water spectrum has the general shape of an isotropic Raman bulk water spectrum, yet there are important differences. Consistent with Raman and infrared pH data and cluster studies, the broad VSF intensity in the 2900 cm^{-1} (±150 cm^{-1}) region is most likely due to various cluster distribution effects.[23] The broad band from approximately 3000 to 3600 cm^{-1} is assigned to the broad distribution of OH hydrogen-bonding stretching modes in which the oxygen is tetrahedrally coordinated. [24−29] The energy region from ~3000 to 3250 cm^{-1} is attributed to the intermolecular coupling of the water molecule symmetric stretch vibrations of the hydrogen-bonding network. This region is dominated by overlapping OH symmetric stretch transitions, ν_1. The higher energy broad band region (~3250−3500 cm^{-1}) is assigned to weaker coupling of the water molecule stretching modes that encompass both ν_1 (OH symmetric stretch) and to a lesser extent, ν_3 (OH asymmetric stretch) vibrational modes. We observe a slight decrease in VSF intensity centered at ~3250 cm^{-1}. In IR and Raman bulk water studies this has been attributed to a Fermi resonance of the ν_1 OH stretching modes with the overtone OH bending modes, $2\nu_2$,[29] or to the isosbestic point postulated to exist for bulk water.[25,30,31] The distinct peak at 3705 cm^{-1} is assigned to the dangling OH bond of water molecules that straddle the interface with one OH bond directed into the vapor phase and the other interacting with the liquid phase. The terminal hydrogen of the dangling $OH_{(da)}$ bonds is not involved in hydrogen bonding to other condensed phase molecules and has also been referred to as the free OH.[15] The shoulder at ~3760 cm^{-1} is assigned to the asymmetric stretch (AS) of the interfacial vapor state water species. The detection of the vapor state species has been discussed in a previous paper.[12,32]

In addition to comparison of surface spectra with bulk Raman and infrared spectra, it is important to compare our VSF spectra with the surface water VSF spectra obtained in other studies. There have been several SSP (out-of-plane) VSF spectra from air/water interfaces published.[13−22] Although these published VSF spectra have general similarities, there are some notable differences, as might be expected from the different laser systems and normalizing procedures used. In the region from 2900 to 3600 cm^{-1}, our VSF spectrum of surface water is similar to VSF surface water spectra published by Shen and co-workers,[13−15] which also shows intensity in the 2900 cm^{-1} region, the inflection region near 3250 cm^{-1}, and a relatively large intensity contribution in the 3190 cm^{-1} region. Although the shape is generally similar, we observe a sharper peak intensity at 3190 cm^{-1}. Shultz and co-workers using a nanosecond laser system observe this peak at 3150 cm^{-1}.[16−19] The SF intensity drop to nearly zero observed at 3220 cm^{-1} by Shultz and co-workers[16−19] is not observed in either our work or the studies by Shen and co-workers.[13−15]

There are also similarities and differences of the VSF spectra in the free OH region (~3700 cm^{-1}) from different groups. In the $OH_{(da)}$ (free OH) bond region, we observe this peak at 3705 cm^{-1} (±6 cm^{-1}). For this work the infrared frequency was carefully calibrated for this spectral assignment with the details given in the Experimental Section. This free OH assignment is in reasonable agreement with Buch and Devlin[26,33] in which

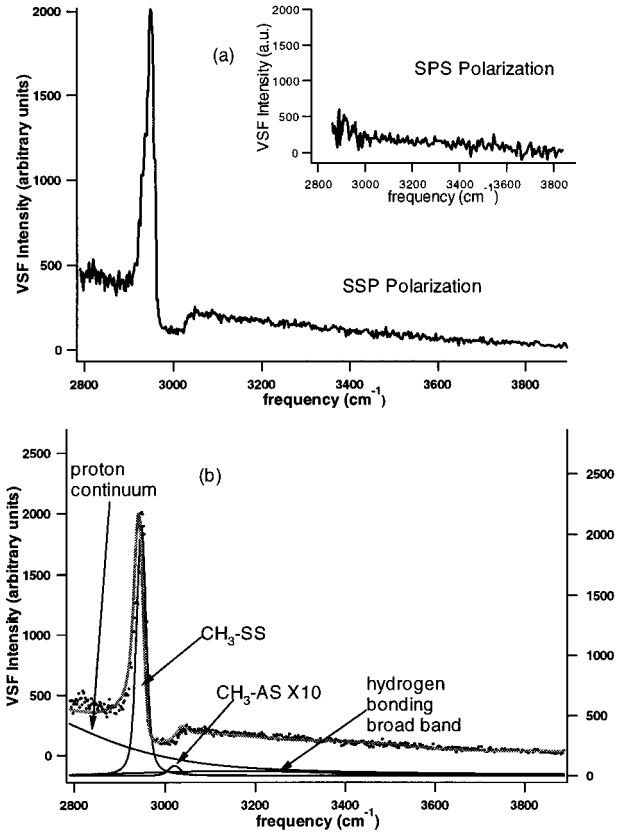

Figure 3. (a) SSP VSF spectrum of the surface of neat MSA which includes the CH_3(SS) at 2947 cm^{-1} and the broad MSA proton continuum. Inset: SPS (in-plane) VSF spectrum of the surface of neat MSA. (b) Fit to the data taking into account the relative VSF phase. Data and fit (left axis) have been offset by 200 units for clarity. The destructive interference (opposing phases) between the CH_3(SS) and the CH_3(AS) is clearly observed between 2950 and 3025 cm^{-1}.

the $OH_{(da)}$ mode is observed at 3696 and 3720 cm^{-1} for 3- and 2-coordinate surface water molecules for amorphous ice surfaces. The literature is somewhat scattered for the free OH assignment from VSF spectra of the vapor/water interface, for which assignments range from 3670 to 3710 cm^{-1},[13−22] yet all results agree reasonably within this range. VSFS intensities differ for the free OH region depending on the laser system utilized, and differences are easily explained by laser pulse temporal dephasing. For our 2 ps laser system in the 3700 cm^{-1} (∼2.7 μm) region the pulse undergoes free induction decay as a result of interaction with water vapor in the atmosphere (discussed in Gragson et al.[8] and Crowell et al.[34]), which redistributes a portion of the energy into surrounding frequencies and dephases the temporal coherence of the beam in this wavelength region. This redistribution of energy results in a smaller than expected peak intensity for the 3705 cm^{-1} vibrational resonance in our VSF spectra, which cannot be accounted for by simply normalizing to the infrared intensity. Consequently, the smaller absolute height of the 3705 cm^{-1} peak is an artifact of the laser and OPA system. From a longer 20 ps pulse, this effect is lessened and with the use of a nanosecond laser, the effects of free induction decay should not be an issue.

III. VSF Spectra of Neat MSA and MSA Solutions. Figure 3a is the VSF spectrum of the neat MSA (99+%) surface. The data was taken with SSP polarizations. The peak fit at 2947 cm^{-1} (±6 cm^{-1}) is assigned to the methyl symmetric stretch (CH_3(SS)). The SF response from the methyl asymmetric stretch (CH_3(AS)) is present but is less obvious. Fits to the data shown in Figure 3b place the AS mode at 3032 cm^{-1}, which is close to that obtained for bulk MSA as measured by Raman and IR (3032 and 3036 cm^{-1}, respectively).[35] The VSF response from the CH_3(AS) and to a lesser extent the broad underlying bands, destructively interfere with the SF response from the CH_3(SS), resulting in an observed decrease in the SF intensity in the 2950−3025 cm^{-1} region. By mathematically transforming the hyperpolarizability elements of the SS and the AS of the methyl group of MSA from molecular coordinates to the laboratory coordinate system via Euler angle rotations, it has been shown previously that the SF response from the SS and the AS of CH modes from methyl groups of C_{3v} symmetry are of opposite phase.[36−38] That is what is observed here. This interference effect coupled with the 85 cm^{-1} peak to peak separation of modes results in the square-shaped intensity drop that is observed in the VSF spectra of MSA solutions shown in Figures 3−5. The shape of the distortion is dependent on the frequency separation of the modes; i.e., smaller frequency separations result in observed sharper dips rather than square intensity drops. The CH_3(AS) is small as shown in Figure 3b, but has a profound impact on the shape of the spectrum.

Underlying the spectral features just discussed is a broad continuum of VSF intensity that extends over the full range observed here. This broad VSF intensity extending from 2800 cm^{-1} to almost 3800 cm^{-1} is attributed to two different sources: the MSA proton continuum band and the hydrogen-bonding bands of surface H_2O discussed in subsection II. Since MSA is a strong acid, it continually undergoes dissociation and association of its acidic proton, which gives rise to the observed continuum shown from 2800 cm^{-1} to past 3400 cm^{-1}. Similar continua have been observed in infrared and Raman spectra of condensed phase acids.[39] Strong acids can be differentiated spectroscopically by their proton continuum, which is always broad yet unique to the acid. Proton continua have been also clearly observed in infrared spectra of liquid MSA and sulfuric acid.[35,40,41] This broad band for surface neat MSA (pK_a of −1.9[41]) begins before 2800 cm^{-1} (estimated peak fit at 2500 cm^{-1}) and extends and decreases uniformly to beyond 3400 cm^{-1}.

To determine the orientation of the MSA molecule at the surface of neat MSA, we have conducted VSFS polarization experiments. For the neat MSA, although we observed a broad SPS VSF intensity, there are no observed sharp resonances for the SPS (in-plane) CH_3(SS) intensity as shown in the inset of Figure 3a. (Low signal-to-noise levels in the SPS spectra are evident in the lower energy region and are due to lower IR energies coupled with low SPS intensity.) From the SSP and the SPS spectra, the distribution of angles for the CH_3 group of MSA is calculated to be 0−60° from the surface normal (see Wolfrum et al.[36] for VSF calculation methods). Additionally, the observed VSF SSP (out-of-plane) intensity of the CH_3(AS) is small as is shown in Figure 3b. This is indicative of a CH_3 axis oriented parallel to the surface normal suggesting a narrower angle distribution of the surface MSA. Combining this calculated orientation with the thermodynamic arguments of subsection I, the surface MSA are placed with their methyl group symmetry axes on average pointing away from the solution surface into the gas phase and the SO_3^- moieties solvated in the solution.

The surface of aqueous solutions of differing MSA concentrations have been examined to provide further insight into the structure of surface MSA as well as the effect of MSA on the hydrogen bonding of surface water. The SSP VSF spectra in Figure 4a,b were taken of 0.02, 0.03, and 0.10 bulk mole fraction methanesulfonic acid (mf MSA) solutions, respectively. For ease of comparison with each other, the MSA spectra in Figure 4a

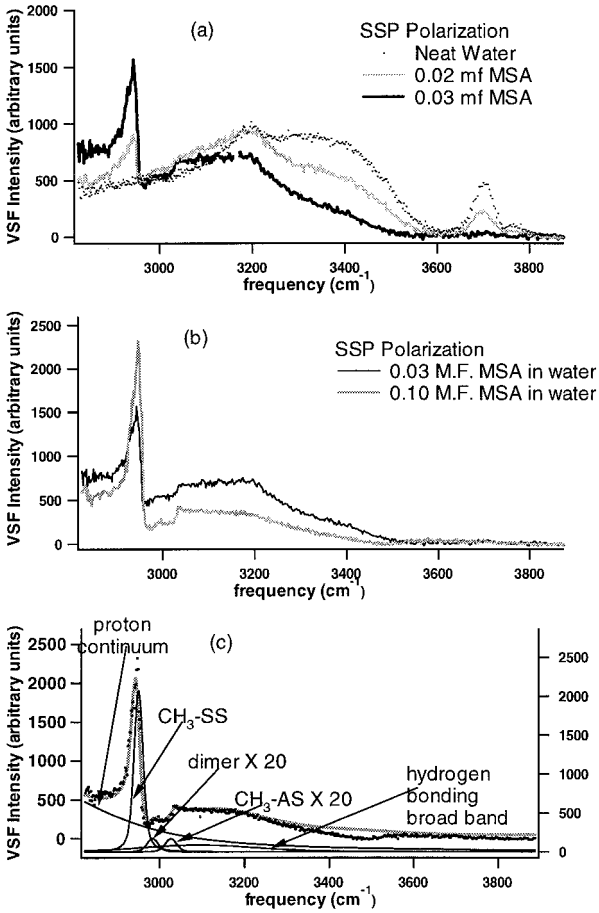

Figure 4. (a) SSP VSF spectra of the surface of 0.02 and 0.03 mf MSA in water. The neat surface water spectrum is shown for comparison. Note the depletion of the free OH with increasing MSA concentration and that the hydrogen-bonding region (3000−3500 cm^{-1}) is significantly changing in shape and frequency distribution with increasing MSA concentration. (b) SSP VSF spectrum of the surface of 0.10 mf MSA. The 0.03 mf MSA is shown for ease of comparison. (c) Fit to the 0.1 mf MSA SSP VSF spectrum. Data and fit (left axis) have been offset by 200 units for clarity.

are superimposed on the VSF spectra of neat water. We observe that the CH_3(SS) peak fit at 2947 cm^{-1} increases in intensity with increasing MSA concentration for these low-concentration solutions. The areas of the CH_3(SS) peaks were fit to a Voigt function and the square root of this area was compared relative to each solution. Shown in Figure 4c is the fit to the 0.1 mf MSA spectra which illustrates this procedure. The increase in number density calculated from the square root of the VSF intensity is consistent with the increase in number density from the surface tension measurements. Comparison of the CH_3(SS) intensity in the 0.1 mf spectrum with the pure MSA spectrum (Figures 4b and 3a) is complicated by the interference between the CH_3 modes, the underlying proton continuum, and water hydrogen-bonding bands for the aqueous solutions. Nevertheless, for all concentrations studied here, the CH_3(SS) peak does not shift in energy, and thus the orientation of the CH_3 groups does not appear to be changing although the shape of the distribution function itself may be altered. Frequency shifts of methyl moieties were observed for similar VSF studies of dimethyl sulfoxide and were attributed to increased crowding at the interface and a subsequent change in molecular orientation.[1] The apparent broadening of the CH_3 peak as water is added indicates a larger number of environments for the surface of the MSA solutions as opposed to neat MSA surfaces. The lack of observed VSFS frequency shifts for the well-resolved CH_3(SS) peak of MSA and its interference edge strongly supports that although the surface environment and surface concentration are changing, at low bulk concentrations of MSA, the average orientation of the surface MSA is not.

The square-shaped intensity drop first observed in Figure 3 (neat MSA) from a destructive interference between the CH_3(SS) and the CH_3(AS) is significantly distorted in the lower concentration MSA spectra. The effect is clearest in the 0.10 mf spectrum of Figure 4b, although it is also evident in the 0.02 and the 0.03 mf MSA solution spectra shown in Figure 4a,b. Accompanying this intensity drop is the asymmetric shape of the CH_3(SS), with a much sharper drop on the high-energy side of the spectrum. Within the square-shaped intensity drop, we observe a small peak at ∼2980 cm^{-1}. There is evidence in gas and condensed phase studies that MSA dimer species ($CH_3SO_3-H-O_3SCH_3$) would give rise to a resonance at 2977 cm^{-1}.[35] In the peak fit shown in Figure 4c, a small 2980 cm^{-1} peak has been included in the fit, but we have also been able to reproduce a similar small peak from changing the surrounding peak parameters in this region without including the 2980 cm^{-1} peak. Thus, with the fitting calculations taking into account the VSF phase information, we cannot say with certainty that the surface MSA dimer exists at the surface of the 0.1 mf MSA solution. If the surface MSA dimer species does exist, the small peak intensity suggests that its surface concentration may be low.

In Figure 4a,b, additional significant spectral features are observed that provide information about the structure of water at the surface of these MSA solutions. In the region from 2800 to 3050 cm^{-1}, we attribute the increase in intensity with increased MSA concentration to an increase in protonated water species (H_3O^+ or $H_5O_2^+$) [39,42] present as the solution concentration becomes more highly acidic. Additionally, the entire hydrogen bonding and dangling OH region from 3000 to 3800 cm^{-1} is significantly affected by small increases in the MSA concentration. The increasing presence of surface MSA causes an overall shift in OH intensity toward the red. This signifies that MSA enhances the coordination between interfacial water molecules. The observed large intensity shift to lower energies in the spectra relative to the neat water surface indicates that the oxygens of the MSA are capable of significant hydrogen bonding to the free OH and surface water molecules. Thus, the number of water molecules with weaker coupling of their vibrational stretching modes decreases as the MSA concentration is increased, and the remaining surface water molecules' vibrational modes are more strongly coupled.

Since the MSA anions are surface active as established by both the surface tension and VSFS data, a net negative charge exists at the uppermost portion of the solution surface. The anion's counterpart, the H_3O^+ (or $H_5O_2^+$) cation, is stabilized in the surface region by the ionic interaction with the surface methanesulfonate anions. Thus, there is a resultant electrostatic field formed by these two species at the surface of aqueous MSA solutions producing a tight double layer. Previous VSF studies of negatively charged surfactants have shown large increases in the VSF signal strength from the OH stretching mode of water in the lower energy hydrogen-bonding spectral region.[43] This enhancement is primarily due to the formation of a double layer, effectively extending the interfacial region. Due to the concentrations and ionic strengths in our MSA studies, the relatively thin double layer that is formed does not significantly increase the interfacial depth. We therefore assume that the SF signal is arising only from the surface MSA molecules. While there is

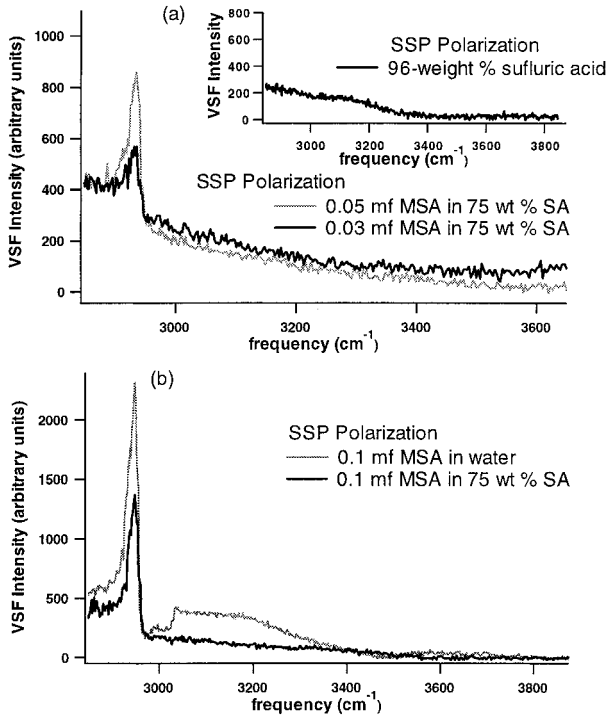

Figure 5. (a) SSP VSF spectra of 0.05 mf MSA and 0.03 mf MSA in 75 wt % sulfuric acid aqueous solution. Inset: SSP VSF spectrum of 96 wt % sulfuric acid. (b) VSF SSP spectrum of 0.10 mf MSA in 75 wt % sulfuric acid aqueous solution. SSP VSF spectrum of 0.10 mf MSA in water is shown here for ease of comparison.

no appreciable VSF intensity increase observed in the surface water region of the MSA solutions, this surface electric field contributes to the strong coupling of the remaining surface water vibrational modes.

In the VSF spectra (Figure 4a,b) the lower intensity of the hydrogen-bonding region and the eventual loss of the free OH peak reflects the lower number density of the surface water, consistent with the surface tension measurements discussed in subsection I. At a bulk concentration of 0.1 mf MSA, the surface MSA:H_2O ratio is 1, as calculated from the surface tension data discussed in subsection I. Given that the square root of the VSF intensity is proportional to the number of orientationally averaged molecules at the surface, we have compared the square root of the free OH peak areas and find that the number of free OH species has been reduced by ∼75% for the 0.02 MSA mf solution surface relative to the free OH number density at the surface of neat water. Another addition of MSA to solution, the 0.03 MSA mf solution, results in a ∼90% depletion of surface free OH species. In the 0.10 mf MSA solution (Figure 4b) the $OH_{(da)}$ peak is below detection limits. These results suggest that close to three-fourths and nine-tenths of the neat water surface $OH_{(da)}$ bonds in the 0.02 and 0.03 mf MSA solutions, respectively, are now hydrogen bonded to an oxygen of either the surface MSA or the remaining surface water, and that by 0.10 MSA mf (0.5 mf_e), there is no evidence of free OH species.

IV. Binary versus Ternary Solutions: Sulfuric Acid, MSA, and Water. Ternary mixtures of sulfuric acid (SA), MSA, and water were studied to help shed light on the surface structures of more complex systems that also have relevance to atmospheric aerosol chemistry. VSF spectra of 0.03 and 0.05 mf MSA in a 75 wt % sulfuric acid (SA) solution (1 SA:2 H_2O molecules) are shown in Figure 5a. (0.03 and 0.05 mf MSA bulk concentrations correspond to approximate bulk ratios of 1 MSA:11 SA:22 H_2O and 1 MSA:6 SA:13 H_2O molecules, respectively.) The sulfuric acid proton continuum shown in Figure 5a dominates the VSF spectra of the 0.03 and 0.05 mf MSA/SA solutions from 2800 to ∼3400 cm^{-1}, and this continuum is comparable in shape and intensity to the surface spectrum of the 96% SA solution shown in the inset of Figure 5a. The CH_3(SS) peak from MSA is observed at 2947 cm^{-1}, riding on top of the continuum intensity. There are no frequency shifts for the CH_3(SS) observed for this mode relative to the pure and binary MSA mixture VSF studies. The sharp decrease in intensity is still observable on the high-frequency side of the CH_3(SS), indicating the destructive interference is still occurring as one would expect. From the VSF spectra of the 0.03 mf and the 0.05 mf MSA/SA solutions, an approximate doubling of the CH_3(SS) VSF intensity is observed, indicating that MSA is partitioning to the surface. This is similar to the partitioning from a purely aqueous solution. (Lack of SPS intensity in experiments probing the CH_3(SS) region indicated that reorientation of the CH_3 is negligible and therefore the square root of the VSF intensity can be directly correlated to surface number density.) In the proton continuum region, we do not observe any distinct features except for possible resonances from the protonated water species, $H_5O_2^+$ and/or H_3O^+.[40,44] What is important to note is that similar interference features are seen in the binary and the ternary solution spectra.

The spectra of MSA in aqueous versus sulfuric acid solutions are compared and shown in Figure 5b in order to understand the differences in surface structure of both MSA and water at these two different surfaces. It is observed from the spectra in Figure 5b that the VSF intensity from the CH_3(SS) peak of MSA is reduced for the ternary mixture, and we do not observe a frequency shift for the CH_3(SS) for the two solutions. The lower CH_3(SS) SSP VSF intensity of the ternary mixture in this region indicates that the MSA surface molecules are being displaced by sulfuric acid and/or sulfuric acid complexes. Reorientation for the CH_3 of MSA in the 0.1 mf MSA/SA solution can be eliminated based on the lack of SPS VSF intensity in our studies of the CH_3(SS) spectral region. The lack of frequency shift for this mode indicates that the local structure of the remaining surface CH_3 groups of MSA is not changing significantly. Clearly, sulfuric acid is more efficient at displacing the methanesulfonic acid from the surface compared to water, and therefore the MSA molecules partition less effectively to the surface in a 75 wt % sulfuric acid aqueous solution.

Conclusions

Methanesulfonic acid adsorption and molecular structure at the surface of aqueous solutions including 75 wt % sulfuric acid have been studied using vibrational sum frequency spectroscopy. Methanesulfonic acid (pK_a −1.9) is a strong acid and below 0.2 mf MSA in aqueous solution, MSA is dissociated from its acidic hydrogen in bulk solution. Surface tension and VSF polarization experimental results indicate that MSA is preferentially adsorbed at the surface of aqueous solutions. The methyl group of MSA is oriented away from the liquid state and this orientation does not change significantly with changing surface concentration. We calculate the angle of the C−S bond that bisects the MSA molecule to be in a distribution from 0° to 60° from the surface normal. Surface water structure in the presence of MSA was also studied using VSFS. In aqueous MSA solutions we find that the MSA partitions to the surface. With small amounts of MSA added to bulk water, the surface water molecule vibrational modes shift to lower energy due to enhanced hydrogen bonding between surface water molecules. With increasing MSA concentration the number of free-OH

bonds decrease as they become coordinated to the oxygen of either surface MSA or remaining surface water molecules, resulting in a red shift of the intensity. In ternary mixtures of MSA, sulfuric acid, and water, sulfuric acid displaces the surface MSA more efficiently than water does from the surface of a binary solution of MSA and water. Thus, heterogeneous chemistry of MSA solutions, which has application to the heterogeneous chemistry of atmospheric aerosols, may be distinctly different from what is observed for the bulk liquid-phase chemistry. This conclusion is based on the fact that heterogeneous chemistry begins with surface adsorption. A highly oriented methyl barrier at the surface of a solution, and an altered surface water structure depleted in surface free OH bonds, will influence gas phase adsorption character and thereby may alter reaction pathways.

Acknowledgment. The authors acknowledge the National Science Foundation (CHE-9725751) for support of the air/water studies, the Department of Energy (DE-FG06-86ER45273) for support of the MSA studies, and the Office of Naval Research for equipment funding.

References and Notes

(1) Davis, D.; Chen, G.; Kasibhatla, P.; Jefferson, A.; Tanner, D.; Eisele, F.; Lenschow, D.; Neff, W.; Berresheim, H. *J. Geophys. Res.* **1998**, *103*, 1657.
(2) Schwartz, S. E.; Andreae, M. O. *Science* **1996**, *272*, 1121.
(3) Charlson, R. J.; Lovelock, J. E.; Andreae, M. O.; Warren, S. G. *Nature* **1987**, *326*, 655.
(4) Charlson, R. J.; Schwartz, S. E.; Hales, J. M.; Cess, R. D.; Coakley, J., J. A.; Hansen, J. E.; Hofmann, D. J. *Science* **1992**, *255*, 423.
(5) De Bruyn, W. J.; Shorter, J. A.; Davidovits, P.; Worsnop, D. R.; Zahniser, M. S.; Kolb, C. E. *J. Geophys. Res.* **1994**, *99*, 16, 927.
(6) Richter, L. J.; Petralli-Mallow, T. P.; Stephenson, J. C. *Opt. Lett.* **1998**, *23*, 1594.
(7) Vogel, A.; Noack, J.; Nahen, K.; Theisen, D.; Busch, S.; Parlitz, U.; Hammer, D. X.; Noojin, G. D.; Rockwell, B. A.; Birngruber, R. *Appl. Phys. B, Lasers Opt.* **1999**, *68*, 271.
(8) Gragson, D. E.; McCarty, B. M.; Richmond, G. L.; Alavi, D. S. *J. Opt. Soc. Am. B* **1996**, *13*, 2075.
(9) Gragson, D. E.; Alavi, D. S.; Richmond, G. L. *Opt. Lett.* **1995**, *20*, 1991.
(10) Allen, H. C.; Gragson, D. E.; Richmond, G. L. *J. Phys. Chem. B* **1999**, *103*, 660-.
(11) Kipling, J. J. Ch. 11. Adsorption at the Liquid−Vapor Interface. In *Adsorption from Solutions of Non-Electrolytes*; Kipling, J. J., Ed.; Academic Press: New York, 1965; p 191.
(12) Allen, H. C.; Raymond, E. A.; Brown, M. G.; Richmond, G. L., submitted for publication.
(13) Miranda, P. B.; Shen, Y. R. *J. Phys. Chem. B* **1999**, *103*, 3292.
(14) Raduge, C.; Pflumio, V.; Shen, Y. R. *Chem. Phys. Lett.* **1997**, *274*, 140.
(15) Du, Q.; Superfine, R.; Freysz, E.; Shen, Y. R. *Phys. Rev. Lett.* **1993**, *70*, 2313.
(16) Schnitzer, C.; Baldelli, S.; Shultz, M. J. *J. Phys. Chem. B* **2000**, *104*, 585.
(17) Schnitzer, C.; Baldelli, S.; Campbell, D. J.; Shultz, M. J. *J. Phys. Chem. A* **1999**, *103*, 6383.
(18) Schnitzer, C.; Baldelli, S.; Shultz, M. J. *Chem. Phys. Lett.* **1999**, *313*, 416.
(19) Simonelli, D.; Baldelli, S.; Shultz, M. J. *Chem. Phys. Lett.* **1998**, *298*, 400.
(20) Baldelli, S.; Schnitzer, C.; Shultz, M. J. *Chem. Phys. Lett.* **1999**, *302*, 157.
(21) Baldelli, S.; Schnitzer, C.; Shultz, M. J.; Campbell, D. J. *Chem. Phys. Lett.* **1998**, *287*, 143.
(22) Baldelli, S.; Schnitzer, C.; Shultz, M. J.; Campbell, D. J. *J. Phys. Chem. B* **1997**, *101*, 10435.
(23) Goss, L. M.; Sharpe, S. W.; Blake, T. A.; Vaida, V.; Brault, J. W. *J. Phys. Chem. A* **1999**, *103*, 8620.
(24) Buch, V.; Devlin, J. P. *J. Chem. Phys.* **1999**, *110*, 3437.
(25) Walrafen, G. E.; Yang, W.-H.; Chu, Y. C. Raman evidence for the clathratelike structure of highly supercooled water. In *Supercooled Liquids*; American Chemical Society: Washington, DC, 1997; Chapter 21, p 287.
(26) Devlin, J. P.; Buch, V. *J. Phys. Chem.* **1995**, *99*, 16534.
(27) Hare, D. E.; Sorenson, C. M. *J. Chem. Phys.* **1990**, *93*, 25.
(28) Whalley, E.; Klug, D. D. *J. Chem. Phys.* **1986**, *84*, 78.
(29) Scherer, J. R. Chapter 3. The vibrational spectroscopy of water. In *Advances in Infrared and Raman Spectroscopy*; Clark, R. J. H., Hester, R. E., Eds.; Heyden: Philadelphia, PA, 1978; Vol. 5, p 149.
(30) Giguere, P. A. *J. Chem. Phys.* **1987**, *87*, 4835.
(31) Walrafen, G. E.; Chu, Y. C. *J. Phys. Chem.* **1995**, *99*, 11225.
(32) Brown, M. G.; Raymond, E. A.; Allen, H. C.; Scatena, L. F.; Richmond, G. L. *J. Phys. Chem. A* **2000**, *104*, 10220.
(33) Buch, V.; Devlin, J. P. *J. Chem. Phys.* **1991**, *94*, 4091.
(34) Crowell, R. A.; Holtom, G. R.; Xie, X. S. *J. Phys. Chem.* **1995**, *99*, 1840.
(35) Chackalackal, S. M.; Stafford, F. E. *J. Am. Chem. Soc.* **1966**, *88*, 4815.
(36) Wolfrum, K.; Laubereau, A. *Chem. Phys. Lett.* **1994**, *228*, 83.
(37) Hirose, C.; Akamatsu, N.; Domen, K. *Appl. Spectrosc.* **1992**, *46*, 1051.
(38) Hirose, C.; Akamatsu, N.; Domen, K. *J. Chem. Phys.* **1992**, *96*, 997.
(39) Zundel, G. In *The Hydrogen Bond II. Structure and Spectroscopy*; Schuster, P., Zundel, G., Sandorfy, C., Eds.; North-Holland Publishing Co.: New York, 1976; Vol. 2, Chapter 15, p 687.
(40) Tomikawa, K.; Kanno, H. *J. Phys. Chem. A* **1998**, *102*, 6082.
(41) Langner, R.; Zundel, G. *J. Chem. Soc., Faraday Trans.* **1998**, *94*, 1805.
(42) Falk, M.; Giguere, P. A. *Can. J. Chem.* **1957**, *35*, 1195.
(43) Gragson, D. E.; McCarty, B. M.; Richmond, G. L. *J. Am. Chem. Soc.* **1997**, *119*, 6144.
(44) Habeeb, M. M. *Appl. Spectrosc. Rev.* **1997**, *32*, 103.